Chapter 28

# Control of Doubly Fed Induction Generators under Balanced and Unbalanced Voltage Conditions

Oriol Gomis-Bellmunt* and Adrià Junyent-Ferré

*Centre d'Innovació Tecnològica en Convertidors Estàtics i Accionaments (CITCEA-UPC)*
*Departament d'Enginyeria Elèctrica,*
*Universitat Politècnica de Catalunya,*
*ETS d'Enginyeria Industrial de Barcelona,*
*Av. Diagonal, 647, Pl. 2. 08028 Barcelona, Spain*

*IREC Catalonia Institute for Energy Research,*
*Josep Pla, B2, Pl. Baixa. E-08019 Barcelona, Spain*
**oriol.gomis@upc.edu*

The present chapter presents a control technique to deal with the control of doubly fed induction generators under different voltage disturbances. Certain current reference values are chosen in the positive and negative sequences so that the torque and the DC voltage are kept stable during balanced and unbalanced conditions. Both rotor-side and grid-side converters are considered, detailing the control scheme of each converter while considering the effect of the crow-bar protection. The control strategy is validated by means of simulations.

## 28.1 Introduction

Power electronics have motivated an important change in the conception of wind farms and have forced to start thinking about wind power plants. Modern wind power plants are based on doubly fed induction Generators (DFIG) or synchronous generators with full power converters (FPC) while they are required to provide support to the grid voltage and frequency by the different power system operators worldwide.

The current grid codes of most countries where wind power is being massively integrated do not not allow wind farms to disconnect when faults in the main grid

occur. Moreover, in some countries support to the main grid in terms of reactive power is demanded during faults.

The task of controlling the Doubly Fed Induction Generator (DFIG) during a voltage sag is specially challenging, since the stator is directly connected to the grid and therefore the stator voltage cannot be prevented to drop suddenly. In the case of unbalanced voltage sags, there also appears a negative sequence which provokes severe power oscillations. The present chapter describes a control technique[1] to deal with such balanced and unbalanced voltage perturbations.

## 28.2 Nomenclature

The chapter employs the following nomenclature. Vectors are expressed as

- $\mathbf{i}_x$: Current vector $i_{xd} + ji_{xq}$
- $\mathbf{v}_x$: Voltage vector $v_{xd} + jv_{xq}$
- $\mathbf{S}_x$: Power vector $P_x + jQ_x$

Scalar quantities:

- $\lambda$: Flux linkage
- $\Gamma$: Torque
- $E$: DC bus voltage
- $t$: Time
- $\omega_e$: Electrical angular velocity
- $\omega_r$: Rotor electrical angular velocity
- $\omega_m$: Mechanical angular velocity
- $\theta$: Angle
- $s$: Slip
- $P$: Generator number of poles
- $f$: Frequency
- $R_r$: Rotor resistance
- $R_s$: Stator resistance
- $L_r$: Rotor inductance
- $L_s$: Stator inductance
- $M$: Mutual inductance

The first subscript:

- $s$: Stator
- $r$: Rotor
- $c$: Rotor-side converter
- $l$: Grid-side converter

- $z$: Grid
- $f$: Filter

The second subscript:

- $d$: d-axis
- $q$: q-axis
- 0: Non-oscillating component
- *sin*: sin oscillating component
- *cos*: cos oscillating component

Superscripts:

- $*$: Set-point
- $p$: Positive sequence
- $n$: Negative sequence

## 28.3 General Considerations

### 28.3.1 *System under study*

The analyzed system is illustrated in Fig. 28.1. The Doubly Fed Induction Generator (DFIG) is attached to the wind turbine by means of a gearbox separating the fast axis connected to the generator to the slow axis attached to the turbine. The DFIG stator windings are connected directly to the wind farm transformer while the rotor windings are connected to a back-to-back converter shown in Fig. 28.2. The converter is composed by the grid-side converter connected to the grid and the rotor-side converter connected to the wound rotor windings.

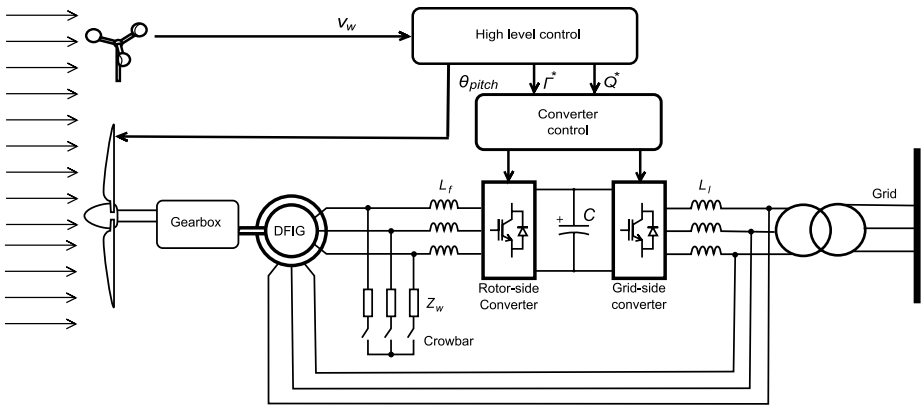


Fig. 28.1. General system scheme.

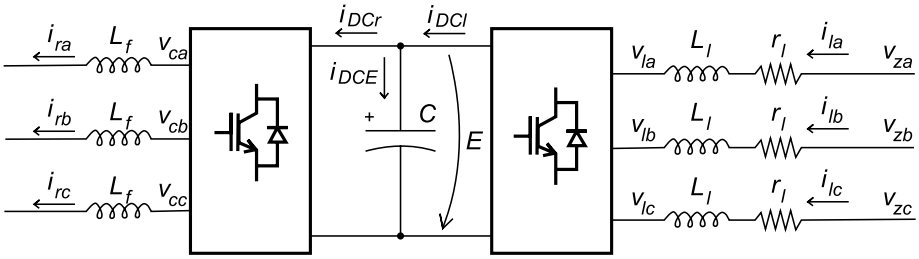


Fig. 28.2. Back to back converter.

The converter set-points are established by the so-called high level controller. It uses the knowledge of the wind speed and the grid active and reactive power requirements, to determine the optimum turbine pitch angle and the torque and reactive power set-points referenced to the converter. The rotor-side converter controls torque and reactive power, while the grid-side converter controls the DC voltage and grid-side reactive power.

Although the back-to-back converter can control both the reactive power injected by the stator by controlling the rotor currents and the reactive power injected directly to the grid with the grid-side converter, it is a common practice to deliver most of the referenced reactive power through the stator while keeping a low or null reactive power set-point in the grid-side converter.

## 28.4 Control of the Doubly Fed Induction Generator under Balanced Conditions

In this section, the classical DFIG control scheme[2] is presented. It was designed for balanced voltage supply.

### 28.4.1 *Analysis*

#### 28.4.1.1 *Grid-side converter*

In the grid-side converter, the DC bus voltage and reactive power references determine the current references, which determine the voltages to be applied in the grid-side.

In a synchronous reference frame, the grid-side voltage equations can be written as:

$$\begin{Bmatrix} v_{zq} \\ v_{zd} \end{Bmatrix} - \begin{Bmatrix} v_{lq} \\ v_{ld} \end{Bmatrix} = \begin{bmatrix} R_l & -L_l\omega_e \\ L_l\omega_e & R_l \end{bmatrix} \begin{Bmatrix} i_{lq} \\ i_{ld} \end{Bmatrix} + \begin{bmatrix} L_l & 0 \\ 0 & L_l \end{bmatrix} \frac{d}{dt} \begin{Bmatrix} i_{lq} \\ i_{ld} \end{Bmatrix}. \quad (28.1)$$

Active and reactive power provided by the grid-side converter can be written as $P_z = \frac{3}{2}(v_{zq}i_{lq} + v_{zd}i_{ld})$ and $Q_z = \frac{3}{2}(v_{zq}i_{ld} - v_{zd}i_{lq})$.

The DC bus voltage can be expressed as:

$$E = E_0 + \frac{1}{C}\int_0^t (i_{DCl} - i_{DCr})\,dt. \tag{28.2}$$

#### 28.4.1.2 *Machine-side converter*

In the rotor side converter, the referenced torque and reactive power determine the current references, which determine the voltages to be applied in the rotor-side.

It is usually assumed that stator and rotor windings are placed sinusoidally and symmetrically, the magnetic saturation effects and the capacitance of all the windings are negligible. The relations between voltages and currents on a synchronous reference *qd* can be written as:

$$\begin{Bmatrix} v_{sq} \\ v_{sd} \\ v_{rq} \\ v_{rd} \end{Bmatrix} = \begin{bmatrix} L_s & 0 & M & 0 \\ 0 & L_s & 0 & M \\ M & 0 & L_r & 0 \\ 0 & M & 0 & L_r \end{bmatrix} \frac{d}{dt} \begin{Bmatrix} i_{sq} \\ i_{sd} \\ i_{rq} \\ i_{rd} \end{Bmatrix} + \begin{bmatrix} R_s & L_s\omega_e & 0 & M\omega_e \\ -L_s\omega_e & R_s & -M\omega_e & 0 \\ 0 & sM\omega_e & R_r & sL_r\omega_e \\ -sM\omega_e & 0 & -sL_r\omega_e & R_r \end{bmatrix} \begin{Bmatrix} i_{sq} \\ i_{sd} \\ i_{rq} \\ i_{rd} \end{Bmatrix}. \tag{28.3}$$

Linkage fluxes can be written as:

$$\begin{Bmatrix} \lambda_{sq} \\ \lambda_{sd} \\ \lambda_{rq} \\ \lambda_{rd} \end{Bmatrix} = \begin{bmatrix} L_s & 0 & M & 0 \\ 0 & L_s & 0 & M \\ M & 0 & L_r & 0 \\ 0 & M & 0 & L_r \end{bmatrix} \begin{Bmatrix} i_{sq} \\ i_{sd} \\ i_{rq} \\ i_{rd} \end{Bmatrix}. \tag{28.4}$$

The torque can expressed as:

$$\Gamma_m = \frac{3}{2}PM(i_{sq}i_{rd} - i_{sd}i_{rq}). \tag{28.5}$$

The reactive power yields:

$$Q_s = \frac{3}{2}(v_{sq}i_{sd} - v_{sd}i_{sq}). \tag{28.6}$$

### 28.4.2 *Control scheme*

#### 28.4.2.1 *Grid-side converter*

The grid-side converter control reactive power and DC bus voltage. The $q$ axis may be aligned to the grid voltage allowing active and reactive decoupled control. To control the reactive power, a $i_{ld}$ reference is computed as:

$$i_{ld}^{*} = \frac{2Q_z^{*}}{3v_{zq}}. \tag{28.7}$$

The active power, which is responsible of the evolution of the DC bus voltage is controlled by the $i_{lq}$ component. A linear controller is usually designed to control the DC bus voltage.

The current control is done by the following state linearization feedback:[3]

$$\begin{Bmatrix} v_{lq} \\ v_{ld} \end{Bmatrix} = \begin{Bmatrix} -\hat{v}_{lq} + v_{zq} - L_l\omega_e i_{ld} \\ -\hat{v}_{ld} + L_l\omega_e i_{lq} \end{Bmatrix}, \tag{28.8}$$

where the $\hat{v}_{lq}$ and $\hat{v}_{ld}$ are the output voltages of the current controller. The decoupling leads to:

$$\frac{d}{dt}\begin{Bmatrix} i_{lq} \\ i_{ld} \end{Bmatrix} = \begin{bmatrix} -\dfrac{R_l}{L_l} & 0 \\ 0 & -\dfrac{R_l}{L_l} \end{bmatrix}\begin{Bmatrix} i_{lq} \\ i_{ld} \end{Bmatrix} + \begin{bmatrix} \dfrac{1}{L_l} & 0 \\ 0 & \dfrac{1}{L_l} \end{bmatrix}\begin{Bmatrix} \hat{v}_{lq} \\ \hat{v}_{qd} \end{Bmatrix}. \tag{28.9}$$

#### 28.4.2.2 *Machine-side converter*

$$i_{sq} = \frac{\lambda_{sq} - Mi_{rq}}{L_s}, \tag{28.10}$$

$$i_{sd} = \frac{\lambda_{sd} - Mi_{rd}}{L_s} = -\frac{Mi_{rd}}{L_s}. \tag{28.11}$$

Thus:

$$\Gamma_m = \frac{3}{2}\frac{PM}{L_s}\lambda_{sq}i_{rd}, \tag{28.12}$$

$$Q_s = \frac{3}{2L_s}(-v_{sq}Mi_{rd} - v_{sd}\lambda_{sq} + Mv_{sd}i_{rq}). \tag{28.13}$$

Orientating the synchronous reference $qd$ with the stator flux vector so that $\lambda_{sd} = 0$, the rotor current references can be computed as:

$$\begin{Bmatrix} i_{rq}^{*} \\ i_{rd}^{*} \end{Bmatrix} = \begin{Bmatrix} \dfrac{\dfrac{2}{3}L_sQ_s^{*} + Mv_{sq}i_{rd} + v_{sd}\lambda_{sq}}{Mv_{sd}} \\ \dfrac{2L_s\Gamma_m^{*}}{3PM\lambda_{sq}} \end{Bmatrix}. \tag{28.14}$$

The control of the current is done by linearizing the current dynamics using the following state feedback:

$$\begin{Bmatrix} v_{rq} \\ v_{rd} \end{Bmatrix} = \begin{Bmatrix} \hat{v}_{rq} + M(\omega_e - \omega_r)i_{sd} + L_r(\omega_e - \omega_r)i_{rd} \\ \hat{v}_{rd} - M(\omega_e - \omega_r)i_{sq} - L_r(\omega_e - \omega_r)i_{rq} \end{Bmatrix}. \tag{28.15}$$

By neglecting stator current transients, the decoupling leads to:

$$\frac{d}{dt}\begin{Bmatrix} i_{rq} \\ i_{rd} \end{Bmatrix} = -\begin{bmatrix} \frac{R_r}{L_r} & 0 \\ 0 & \frac{R_r}{L_r} \end{bmatrix}\begin{Bmatrix} i_{rq} \\ i_{rd} \end{Bmatrix} + \begin{bmatrix} \frac{1}{L_r} & 0 \\ 0 & \frac{1}{L_r} \end{bmatrix}\begin{Bmatrix} \hat{v}_{rq} \\ \hat{v}_{rd} \end{Bmatrix}. \tag{28.16}$$

### 28.4.3 *Current controllers design*

Current controllers can be been designed using the so-called internal mode control (IMC) methodology.[4] The parameters of a Proportional Integral (PI) controller to obtain a desired time constant $\tau$ are obtained as:

$$K_p = \frac{L}{\tau}, \quad K_i = \frac{R}{\tau}. \tag{28.17}$$

The currents and voltages have been limited according to the converter operating limits. PI controllers have been designed with anti-windup in order to prevent control instabilities when the controller exceed the limit values.

Example current loop responses to voltage disturbances are shown in Fig. 28.3.

### 28.4.4 *Crowbar protection*

The so-called crow-bar is connected to avoid overvoltages in the DC bus due to excessive power flowing from the rotor inverter to the grid-side converter, guaranteeing ride-through operation of the generator when voltage sags or other disturbances occur.

The crow-bar is triggered when the DC voltage reaches a threshold $v_{\text{crow}-c}$ and disconnects when it goes below another threshold $v_{\text{crow}-d}$.

During its operation, the rotor-side converter may be disconnected[5] or be kept connected[6] to avoid losing control over the machine.

A DC bus voltage evolution example is shown in Fig. 28.4. It can be seen that the crow-bar protection is connected when the overvoltage occur and that after a transient the DC bus voltage can return to the reference value. The threshold $v_{\text{crow}-c}$ is located at 1180 V and $v_{\text{crow}-d}$ at 1140 V.

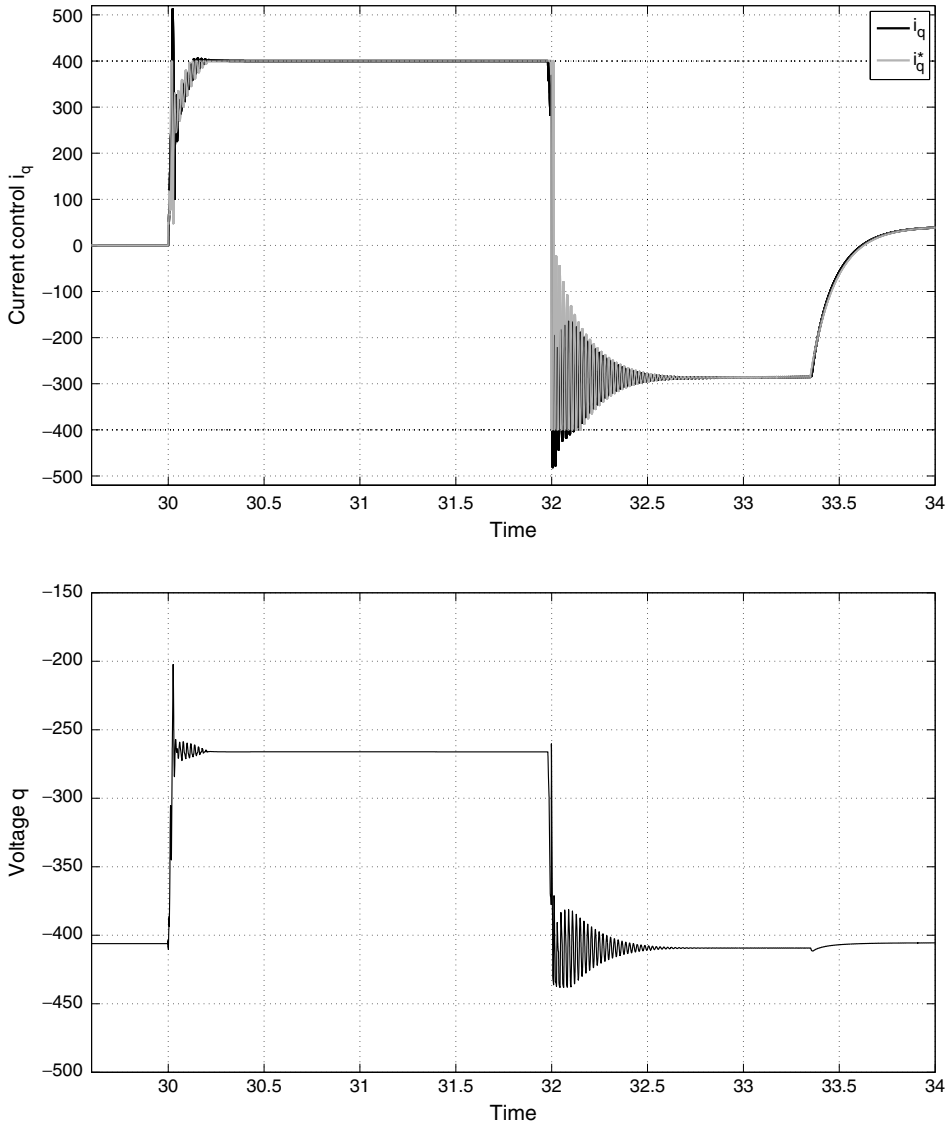


Fig. 28.3. Current loop example.

## 28.5 Control of the Doubly Fed Induction Generator under Unbalanced Conditions

### 28.5.1 *Analysis*

In this section non symmetrical voltage sags are considered. Such unbalanced sags imply negative sequence components in all the relevant quantities. Therefore,

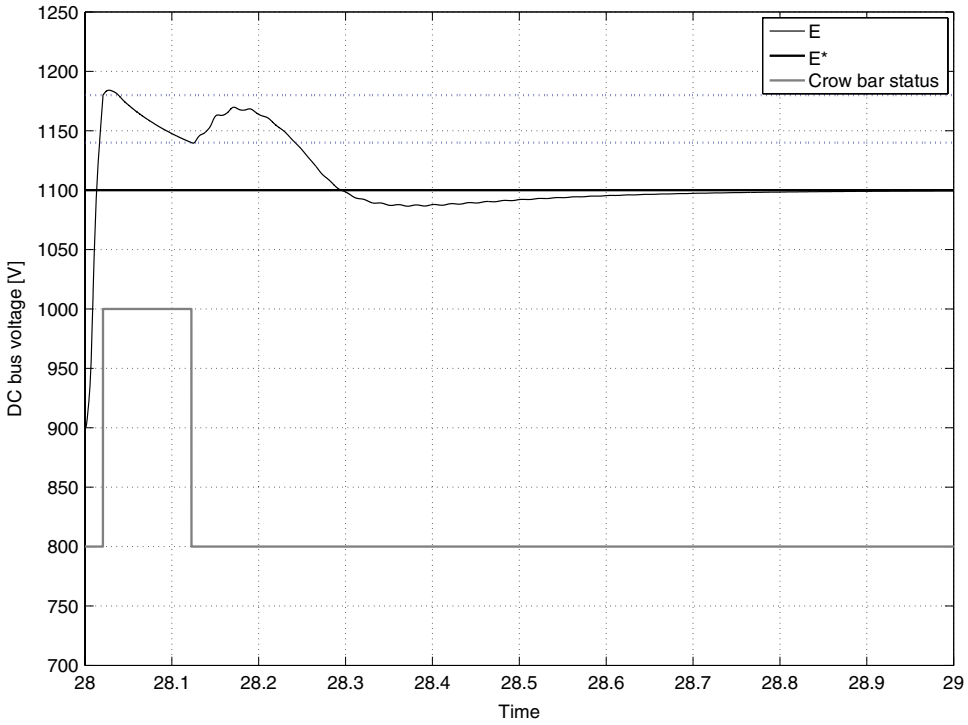


Fig. 28.4. DC bus voltage evolution example.

important oscillations appear in torque, active and reactive power. Such oscillations have a pulsation of $2\omega_e$. Example power and torque oscillations employing the control scheme of the previous Section are shown in Fig. 28.5.

In order to mitigate such oscillations, an approach taking into account the negative sequence quantities is required. The present section analyzes a whole back-to-back converter taking into account both the positive and negative sequence components, and proposes a technique to control optimally both the DC bus voltage and the torque when unbalanced voltage sags occur.

As far as unbalanced systems are concerned, it is useful to express three-phase quantities $x_{abc} = \{x_a, x_b, x_c\}^T$ in direct and inverse components as:

$$\mathbf{x} = e^{j\omega_e t + j\theta_0}\mathbf{x}^p + e^{-j\omega_e t - j\theta_0}\mathbf{x}^n, \tag{28.18}$$

where $\mathbf{x} = \frac{2}{3}(x_a + ax_b + a^2x_c)$, $a = e^{j2\pi/3}$, $\mathbf{x}^p = x_d^p + jx_q^p$ and $\mathbf{x}^n = x_d^n + jx_q^n$.

In the present section, voltages, currents and fluxes are regarded as a composition of such positive and negative sequences.

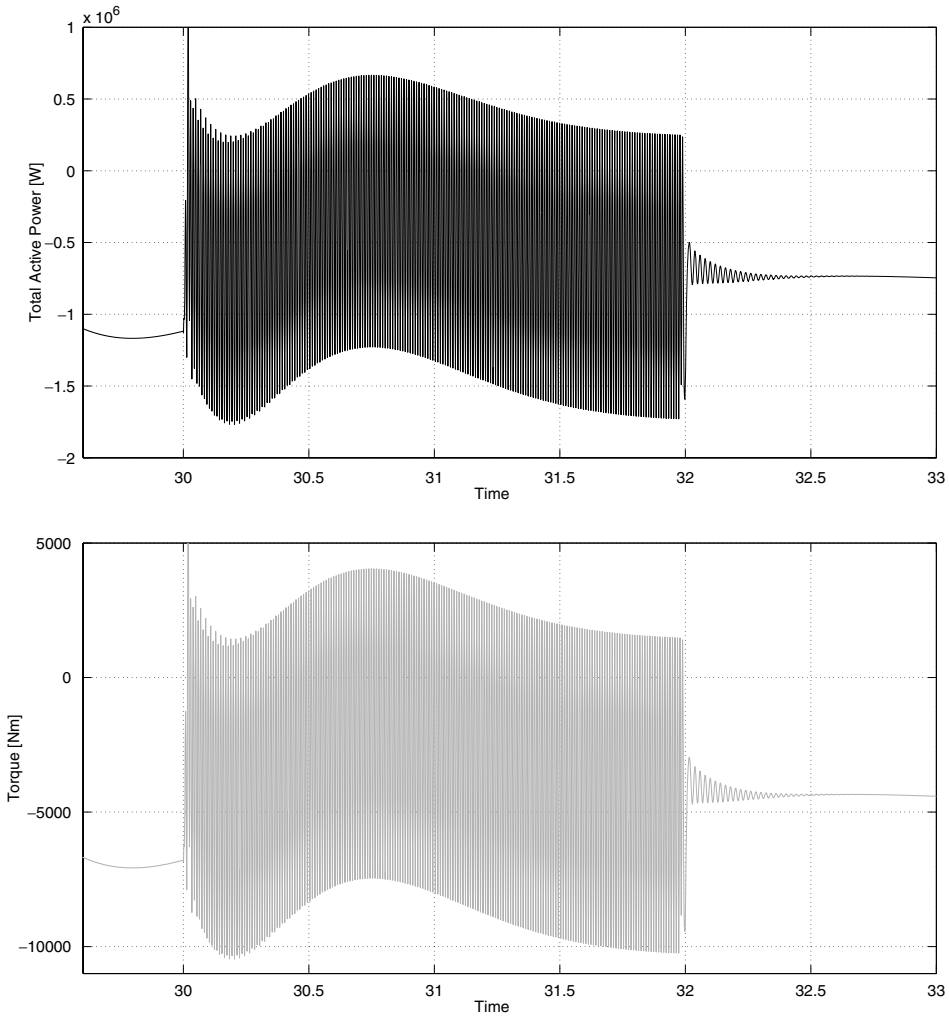


Fig. 28.5. Generator power and torque during an unbalanced voltage sag using conventional control.

#### 28.5.1.1 *Grid-side converter*

Considering two rotating reference frames at $+\omega_e$ and $-\omega_e$, the voltage equations for the positive and negative sequence yield:

$$\mathbf{v}^p_{zqd} - \mathbf{v}^p_{lqd} = (R_l + j\omega_e L_l)\mathbf{i}^p_{lqd} + L_l \frac{d\mathbf{i}^p_{lqd}}{dt}, \tag{28.19}$$

$$\mathbf{v}^n_{zqd} - \mathbf{v}^n_{lqd} = (R_l - j\omega_e L_l)\mathbf{i}^n_{lqd} + L_l \frac{d\mathbf{i}^n_{lqd}}{dt}. \tag{28.20}$$

Active and reactive power can be written:[7]

$$P_l = \frac{3}{2}[P_{l0} + P_{lcos}\cos(2\omega_e t) + P_{lsin}\sin(2\omega_e t)], \tag{28.21}$$

$$Q_l = \frac{3}{2}[Q_{l0} + Q_{lcos}\cos(2\omega_e t) + Q_{lsin}\sin(2\omega_e t)], \tag{28.22}$$

where

$$\begin{Bmatrix} P_{l0} \\ P_{lcos} \\ P_{lsin} \\ Q_{l0} \\ Q_{lcos} \\ Q_{lsin} \end{Bmatrix} = \begin{bmatrix} v_{zd}^p & v_{zq}^p & v_{zd}^n & v_{zq}^n \\ v_{zd}^n & v_{zq}^n & v_{zd}^p & v_{zq}^p \\ v_{zq}^n & -v_{zd}^n & -v_{zq}^p & v_{zd}^p \\ v_{zq}^p & -v_{zd}^p & v_{zq}^n & -v_{zd}^n \\ v_{zq}^n & -v_{zd}^n & v_{zq}^p & -v_{zd}^p \\ -v_{zd}^n & -v_{zq}^n & v_{zd}^p & v_{zq}^p \end{bmatrix} \begin{Bmatrix} i_{ld}^p \\ i_{lq}^p \\ i_{ld}^n \\ i_{lq}^n \end{Bmatrix}. \tag{28.23}$$

It can be noted that both active and reactive power quantity have three different components each, and hence with the four regulable currents $i_{ld}^p$, $i_{lq}^p$, $i_{ld}^n$ and $i_{lq}^n$ only four of such six powers can be controlled.

#### 28.5.1.2 *Machine-side converter*

**Voltage equations.** Considering two rotating reference frames at $+\omega_e$ and $-\omega_e$, the voltage equations for the positive and negative sequence can be obtained as:

$$\begin{Bmatrix} \mathbf{v}_s^p \\ \mathbf{v}_r^p \end{Bmatrix} = \begin{bmatrix} L_s & M \\ M & L_r \end{bmatrix} \frac{d}{dt} \begin{Bmatrix} \mathbf{i}_s^p \\ \mathbf{i}_r^p \end{Bmatrix} + \begin{bmatrix} R_s + jL_s\omega_e & jM\omega_e \\ jM(\omega_e - \omega_r) & R_r + jL_r(\omega_e - \omega_r) \end{bmatrix} \begin{Bmatrix} \mathbf{i}_s^p \\ \mathbf{i}_r^p \end{Bmatrix}, \tag{28.24}$$

$$\begin{Bmatrix} \mathbf{v}_s^n \\ \mathbf{v}_r^n \end{Bmatrix} = \begin{bmatrix} L_s & M \\ M & L_r \end{bmatrix} \frac{d}{dt} \begin{Bmatrix} \mathbf{i}_s^n \\ \mathbf{i}_r^n \end{Bmatrix} + \begin{bmatrix} R_s - j\omega_e L_s & -j\omega_e M \\ +jM(-\omega_e - \omega_r) & R_r + jL_r(-\omega_e - \omega_r) \end{bmatrix} \begin{Bmatrix} \mathbf{i}_s^n \\ \mathbf{i}_r^n \end{Bmatrix}. \tag{28.25}$$

**Stator power expression.** The apparent stator power can be expressed as:

$$\mathbf{S}_s = P_s + jQ_s = \frac{3}{2}\mathbf{v}_s\mathbf{i}_s^*. \tag{28.26}$$

Using Eq. (28.18):

$$\begin{aligned}\mathbf{S}_s &= (e^{j\omega_e t+j\theta_0}\mathbf{v}_s^p + e^{-j\omega_e t-j\theta_0}\mathbf{v}_s^n)((e^{j\omega_e t+j\theta_0})^*\mathbf{i}_s^{p*} + (e^{-j\omega_e t-j\theta_0})^*\mathbf{i}_s^{n*}),\\ \mathbf{S}_s &= \mathbf{v}_s^p\mathbf{i}_s^{p*} + \mathbf{v}_s^n\mathbf{i}_s^{n*} + e^{j2\omega_e t+j2\theta_0}\mathbf{v}_s^p\mathbf{i}_s^{n*} + e^{-j2\omega_e t-j2\theta_0}\mathbf{v}_s^n\mathbf{i}_s^{p*}.\end{aligned} \tag{28.27}$$

Taking into account $\mathbf{x}_s^i = x_{sd}^i + jx_{sq}^i$, and rearranging, it can be written as $\mathbf{S}_s = P_s + jQ_s$, with

$$P_s = \frac{3}{2}[P_{s0} + P_{s\,cos}\cos(2\omega_e t + 2\theta_0) + P_{ssin}\sin(2\omega_e t + 2\theta_0)], \tag{28.28}$$

$$Q_s = \frac{3}{2}[Q_{s0} + Q_{s\,cos}\cos(2\omega_e t + 2\theta_0) + Q_{ssin}\sin(2\omega_e t + 2\theta_0)], \tag{28.29}$$

where

$$\begin{Bmatrix} P_{s0}\\ P_{scos}\\ P_{ssin}\\ Q_{s0}\\ Q_{scos}\\ Q_{ssin}\end{Bmatrix} = \begin{bmatrix} v_{sd}^p & v_{sq}^p & v_{sd}^n & v_{sq}^n\\ v_{sd}^n & v_{sq}^n & v_{sd}^p & v_{sq}^p\\ v_{sq}^n & -v_{sd}^n & -v_{sq}^p & v_{sd}^p\\ v_{sq}^p & -v_{sd}^p & v_{sq}^n & -v_{sd}^n\\ v_{sq}^n & -v_{sd}^n & v_{sq}^p & -v_{sd}^p\\ -v_{sd}^n & -v_{sq}^n & v_{sd}^p & v_{sq}^p\end{bmatrix}\begin{Bmatrix} i_{sd}^p\\ i_{sq}^p\\ i_{sd}^n\\ i_{sq}^n\end{Bmatrix}. \tag{28.30}$$

Substituting stator currents in Eq. (28.30):

$$\begin{Bmatrix} P_{s0}\\ P_{scos}\\ P_{ssin}\\ Q_{s0}\\ Q_{scos}\\ Q_{ssin}\end{Bmatrix} = \frac{1}{L_s}\begin{bmatrix} v_{sd}^p & v_{sq}^p & v_{sd}^n & v_{sq}^n\\ v_{sd}^n & v_{sq}^n & v_{sd}^p & v_{sq}^p\\ v_{sq}^n & -v_{sd}^n & -v_{sq}^p & v_{sd}^p\\ v_{sq}^p & -v_{sd}^p & v_{sq}^n & -v_{sd}^n\\ v_{sq}^n & -v_{sd}^n & v_{sq}^p & -v_{sd}^p\\ -v_{sd}^n & -v_{sq}^n & v_{sd}^p & v_{sq}^p\end{bmatrix}\begin{Bmatrix} \lambda_{sd}^p - Mi_{rd}^p\\ \lambda_{sq}^p - Mi_{rq}^p\\ \lambda_{sd}^n - Mi_{rd}^n\\ \lambda_{sq}^n - Mi_{rq}^n\end{Bmatrix}. \tag{28.31}$$

It can be noted that both active and reactive power quantity have three different components each, and therefore with the four regulable currents $i_{rd}^p$, $i_{rq}^p$, $i_{rd}^n$ and $i_{rq}^n$ only four of the six power quantities can be controlled.

**Rotor power expression.** The apparent rotor power can be expressed as:

$$\mathbf{S}_r = P_r + jQ_r = \frac{3}{2}\mathbf{v}_r\mathbf{i}_r^*, \tag{28.32}$$

$$\begin{aligned}\mathbf{S}_r = \frac{3}{2}&(e^{j(\omega_e-\omega_r)t+j\theta_{r0}}\mathbf{v}_r^p + e^{-j(\omega_e+\omega_r)t-j\theta_{r0}}\mathbf{v}_r^n)\\ &\times (e^{j(\omega_e-\omega_r)t+j\theta_{r0}}\mathbf{i}_r^p + e^{-j(\omega_e+\omega_r)t-j\theta_{r0}}\mathbf{i}_r^n)^*.\end{aligned} \tag{28.33}$$

Using Eq. (28.18):

$$\mathbf{S}_r = \frac{3}{2}[\mathbf{v}_r^p \mathbf{i}_r^{p*} + \mathbf{v}_r^n \mathbf{i}_r^{n*} + e^{j2\omega_e t + 2j\theta_{r0}} \mathbf{v}_r^p \mathbf{i}_r^{n*} + e^{j-2\omega_e t - j2\theta_{r0}} \mathbf{v}_r^n \mathbf{i}_r^{p*}]. \quad (28.34)$$

Taking into account $\mathbf{x}_s^i = x_{sd}^i + jx_{sq}^i$, and rearranging, and analyzing the active rotor power:

$$P_r = \frac{3}{2}[P_{r0} + P_{rcos}\cos(2\omega_e t + 2\theta_{r0}) + P_{rsin}\sin(2\omega_e t + 2\theta_{r0})], \quad (28.35)$$

where

$$\begin{Bmatrix} P_{r0} \\ P_{rcos} \\ P_{rsin} \end{Bmatrix} = \begin{bmatrix} v_{cd}^p & v_{cq}^p & v_{cd}^n & v_{cq}^n \\ v_{cd}^n & v_{cq}^n & v_{cd}^p & v_{cq}^p \\ v_{cq}^n & -v_{cd}^n & -v_{cq}^p & v_{cd}^p \end{bmatrix} \begin{Bmatrix} i_{rd}^p \\ i_{rq}^p \\ i_{rd}^n \\ i_{rq}^n \end{Bmatrix}. \quad (28.36)$$

**Torque expression.** Analogously, electrical torque can be expressed as:

$$\Gamma = \frac{P}{2}\frac{3}{2}[\Gamma_0 + \Gamma_{sin}\sin(2\omega_e t) + \Gamma_{cos}\cos(2\omega_e t)], \quad (28.37)$$

where

$$\begin{Bmatrix} \Gamma_0 \\ \Gamma_{cos} \\ \Gamma_{sin} \end{Bmatrix} = \frac{M}{L_s} \begin{bmatrix} -\lambda_{sq}^p & \lambda_{sd}^p & -\lambda_{sq}^n & \lambda_{sd}^n \\ \lambda_{sd}^n & \lambda_{sq}^n & -\lambda_{sd}^p & -\lambda_{sq}^p \\ -\lambda_{sq}^n & \lambda_{sd}^n & -\lambda_{sq}^p & \lambda_{sd}^p \end{bmatrix} \begin{Bmatrix} i_{rd}^p \\ i_{rq}^p \\ i_{rd}^n \\ i_{rq}^n \end{Bmatrix}. \quad (28.38)$$

### 28.5.2 *Control scheme*

#### 28.5.2.1 *General control structure*

Since there are eight degrees of freedom (the rotor-side currents $i_{rd}^p, i_{rq}^p, i_{rd}^n, i_{rq}^n$ and the grid-side currents $i_{ld}^p, i_{lq}^p, i_{ld}^n, i_{lq}^n$), eight control objectives may be chosen. This implies that it is not possible to eliminate all the oscillations provoked by the unbalance. In this work, the main objective is to ride through voltage dips. Hence, it is important to keep the torque and DC bus voltage as constant as possible and to keep reasonable values of reactive power. To this end it has been chosen to determine the currents to keep certain values of $\Gamma_0^*$, $\Gamma_{cos}^*$, $\Gamma_{sin}^*$, $Q_{s0}^*$ for the rotor-side converter and $P_{l0}^*$, $P_{lcos}^*$, $P_{lsin}^*$ and $Q_{l0}^*$ for the grid-side converter. It can be noted that $P_{l0}^*$, $P_{lcos}^*$ and $P_{lsin}^*$ are directly linked to the DC bus voltage.

The DC voltage $E$ is regulated by means of a linear controller whose output is the power demanded to the grid-side converter. Considering the power terms $P_{r0}$, $P_{rcos}$ and $P_{rsin}$ in the rotor side converter, $P_{r0}$ can be regarded as the average

power delivered, while $P_{rcos}$ and $P_{rsin}$ are the rotor power oscillating terms. Such terms will cause DC voltage oscillations, and hence they can be canceled by choosing:

$$P^*_{lcos} = P_{rcos} P^*_{lsin} = P_{rsin}. \tag{28.39}$$

$P_{l0}$ can be computed as:

$$P^*_{l0} = P_{r0} + P^*_E, \tag{28.40}$$

where $P^*_E$ is the output of the DC voltage linear controller.

The grid reference currents can be computed from Eqs. (28.23), (28.36), (28.39) and (28.40) as:

$$\begin{Bmatrix} i^{p*}_{ld} \\ i^{p*}_{lq} \\ i^{n*}_{ld} \\ i^{n*}_{lq} \end{Bmatrix} = \begin{bmatrix} v^p_{zd} & v^p_{zq} & v^n_{zd} & v^n_{zq} \\ v^n_{zd} & v^n_{zq} & v^p_{zd} & v^p_{zq} \\ v^n_{zq} & -v^n_{zd} & -v^p_{zq} & v^p_{zd} \\ v^p_{zq} & -v^p_{zd} & v^n_{zq} & -v^n_{zd} \end{bmatrix}^{-1} \left( \begin{Bmatrix} P_E \\ 0 \\ 0 \\ Q^*_{l0} \end{Bmatrix} + \begin{bmatrix} v^p_{cd} & v^p_{cq} & v^n_{cd} & v^n_{cq} \\ v^n_{cd} & v^n_{cq} & v^p_{cd} & v^p_{cq} \\ v^n_{cq} & -v^n_{cd} & -v^p_{cq} & v^p_{cd} \\ 0 & 0 & 0 & 0 \end{bmatrix} \begin{Bmatrix} i^p_{rd} \\ i^p_{rq} \\ i^n_{rd} \\ i^n_{rq} \end{Bmatrix} \right). \tag{28.41}$$

The rotor reference currents can be computed from Eqs. (28.38) and (28.31) as:

$$\begin{Bmatrix} i^{p*}_{rd} \\ i^{p*}_{rq} \\ i^{n*}_{rd} \\ i^{n*}_{rq} \end{Bmatrix} = \begin{bmatrix} -\lambda^p_{sq} & \lambda^p_{sd} & -\lambda^n_{sq} & \lambda^n_{sd} \\ \lambda^n_{sd} & \lambda^n_{sq} & -\lambda^p_{sd} & -\lambda^p_{sq} \\ -\lambda^n_{sq} & \lambda^n_{sd} & -\lambda^p_{sq} & \lambda^p_{sd} \\ -v^p_{sq} & v^p_{sd} & -v^n_{sq} & v^n_{sd} \end{bmatrix}^{-1} \times \begin{Bmatrix} \frac{2}{P}\frac{2}{3}\frac{L_s}{M}\Gamma^*_0 \\ \frac{2}{P}\frac{2}{3}\frac{L_s}{M}\Gamma^*_{cos} \\ \frac{2}{P}\frac{2}{3}\frac{L_s}{M}\Gamma^*_{sin} \\ \frac{1}{M}[L_s Q^*_{s0} - \lambda^p_{sd} v^p_{sq} + \lambda^p_{sq} v^p_{sd} - \lambda^n_{sd} v^n_{sq} + \lambda^n_{sq} v^n_{sd}] \end{Bmatrix}. \tag{28.42}$$

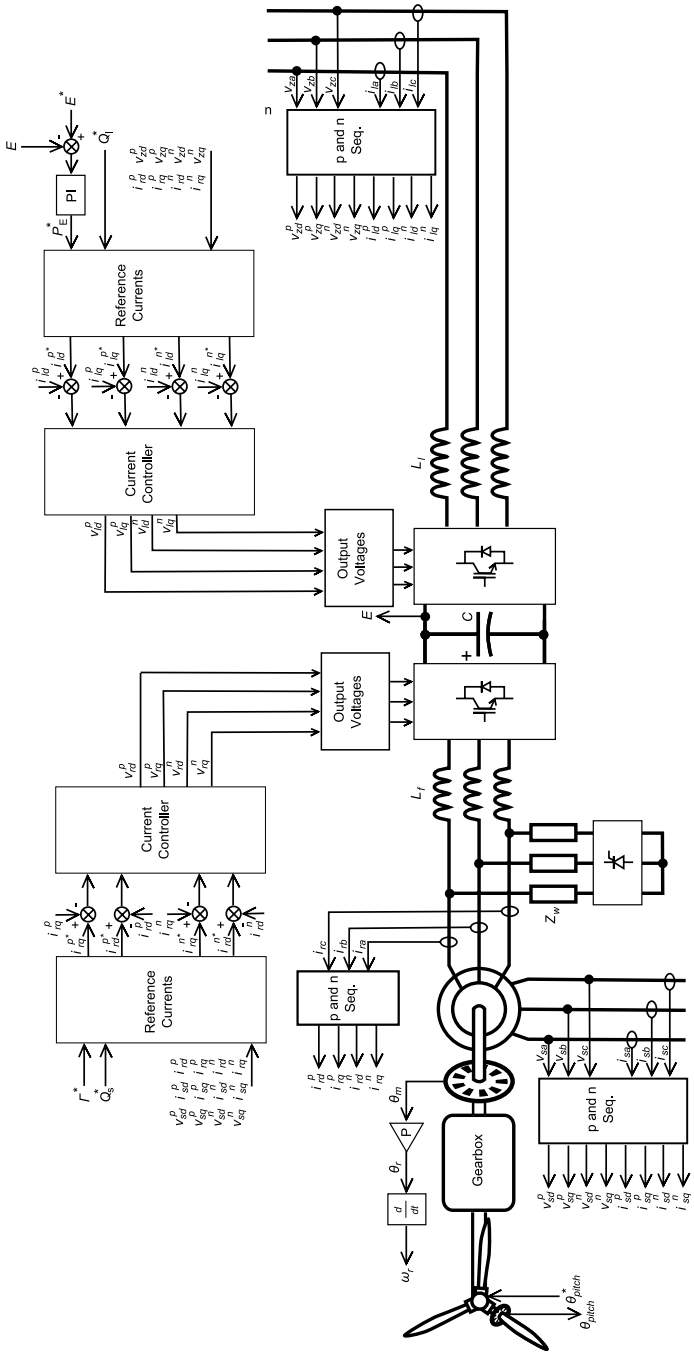


Fig. 28.6. General control scheme.

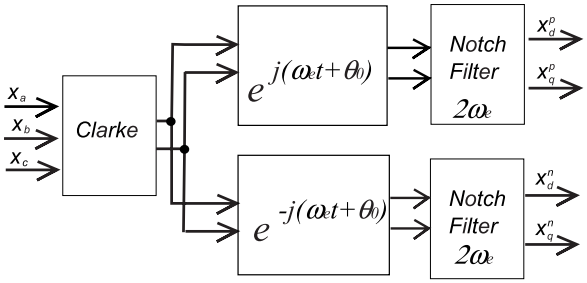


Fig. 28.7. Positive and negative components calculation.

#### 28.5.2.2 *Positive and negative components calculation*

The positive and negative sequence components calculation is done by doing the Clarke transformation, rotating either $e^{j\omega_e t}$ or $e^{-j\omega_e t}$ and finally applying a notch-filter at $2\omega_e$ to eliminate the opposite sequence. The technique is exemplified in Fig. 28.7. For the rotor voltages and currents, the rotation applied is either $e^{j(\omega_e-\omega_r)t}$ or $e^{j(-\omega_e-\omega_r)t}$.

#### 28.5.2.3 *Reference orientation*

The rotating references have been aligned with the stator voltage so that $v_{sq}^p = 0$. Nevertheless, $v_{sq}^p$ has not been substituted in previous expressions for the sake of describing general results. Orientation may be done computing the required $\theta_0$ assuming a constant $\omega_e$ or using a Phase Locked Loop (PLL) to determine both $\omega_e$ and $\theta_0$.

#### 28.5.2.4 *Controllers linearization and tuning*

**Grid-side.** Similarly to the balanced case the control of the current is done by linearizing the current dynamics using:

$$\hat{\mathbf{v}}_{zqd}^p = \mathbf{v}_{zqd}^p - \mathbf{v}_{lqd}^p - j\omega_e L_l \mathbf{i}_{lqd}^p, \tag{28.43}$$

$$\hat{\mathbf{v}}_{zqd}^n = \mathbf{v}_{zqd}^n - \mathbf{v}_{lqd}^n + j\omega_e L_l \mathbf{i}_{lqd}^n. \tag{28.44}$$

The decoupled system yields:

$$\frac{d\mathbf{i}_{lqd}^p}{dt} = \frac{\hat{\mathbf{v}}_{zqd}^p - R_l \mathbf{i}_{lqd}^p}{L_l}, \tag{28.45}$$

$$\frac{d\mathbf{i}_{lqd}^n}{dt} = \frac{\hat{\mathbf{v}}_{zqd}^n - R_l \mathbf{i}_{lqd}^n}{L_l}. \tag{28.46}$$

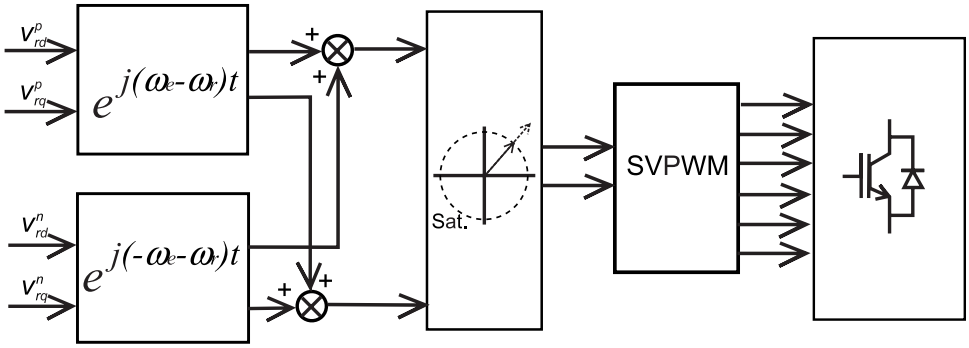


Fig. 28.8. Output voltage calculation: Rotor-side converter example.

**Rotor-side.** Analogously to the balanced case

$$\hat{\mathbf{v}}_r^p = \mathbf{v}_r^p - jM(\omega_e - \omega_r)\mathbf{i}_s^p - jL_r(\omega_e - \omega_r)\mathbf{i}_r^p, \tag{28.47}$$

$$\hat{\mathbf{v}}_r^n = \mathbf{v}_r^n - jM(-\omega_e - \omega_r)\mathbf{i}_s^n - jL_r(-\omega_e - \omega_r)\mathbf{i}_r^n. \tag{28.48}$$

Neglecting the derivative of stator currents, the decoupled system yields:

$$\frac{d\mathbf{i}_r^p}{dt} = \frac{\hat{\mathbf{v}}_r^p - R_r\mathbf{i}_r^p}{L_r}, \tag{28.49}$$

$$\frac{d\mathbf{i}_r^n}{dt} = \frac{\hat{\mathbf{v}}_r^n - R_r\mathbf{i}_r^n}{L_r}. \tag{28.50}$$

28.5.2.5 *Output voltage calculation*

The output voltages calculation is done by summing the resulting positive sequence and negative sequence voltages in the stationary reference frame. For the line-side:

$$\mathbf{v}_l = e^{j\omega_e t}\mathbf{v}_l^p + e^{-j\omega_e t}\mathbf{v}_l^n. \tag{28.51}$$

For the rotor-side:

$$\mathbf{v}_r = e^{j(\omega_e-\omega_r)t}\mathbf{v}_r^p + e^{j(-\omega_e-\omega_r)t}\mathbf{v}_r^n. \tag{28.52}$$

The resulting voltages are limited according to the converter rating. The final voltages can be applied using standard SVPWM techniques. The technique is exemplified for rotor-side converter case in Fig. 28.8.

## 28.6 Simulation Results

The proposed control scheme have been evaluated by means of simulations with one balanced and one unbalanced voltage sag.

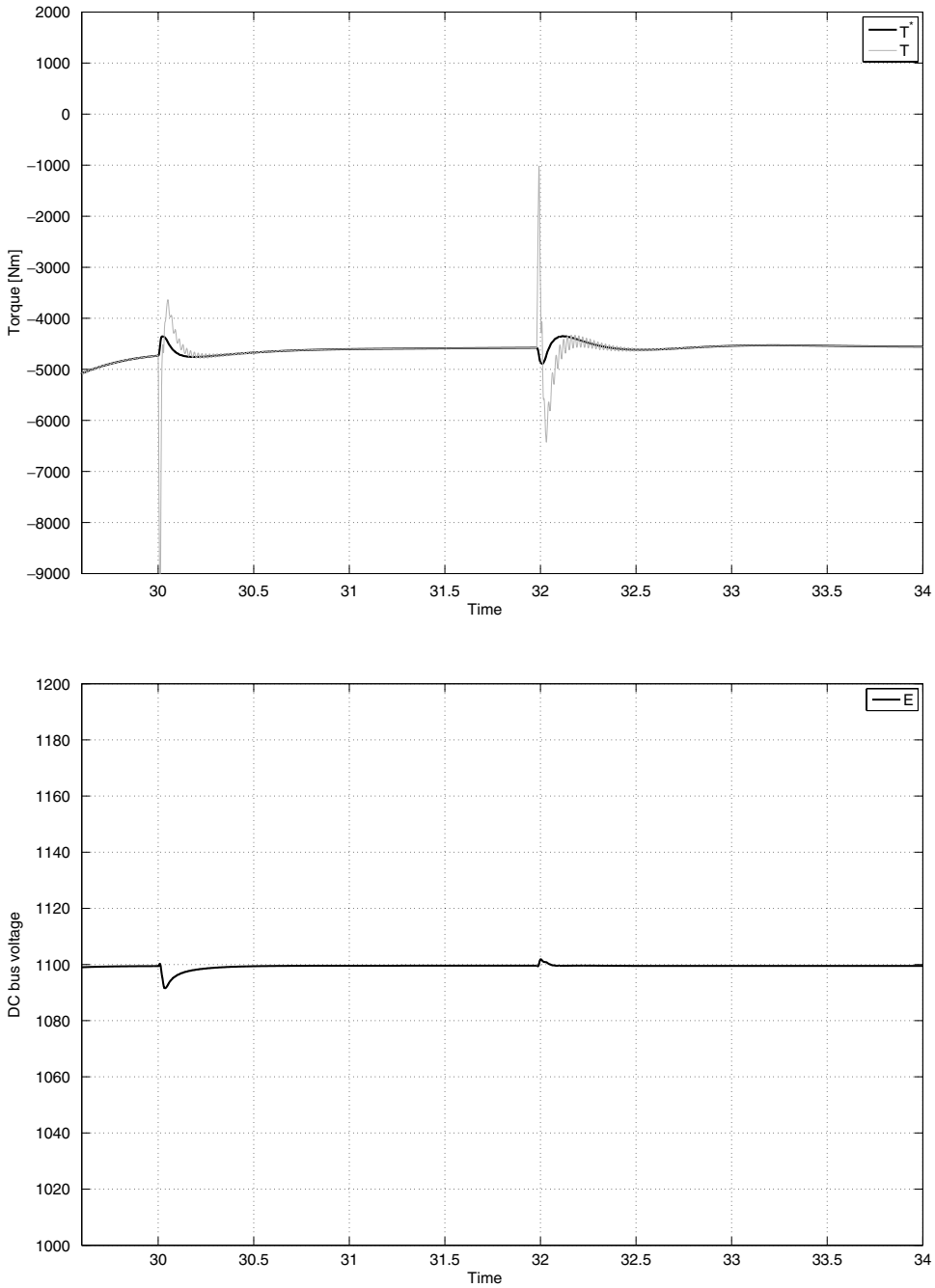


Fig. 28.9. Torque and DC bus response to a balanced voltage sag.

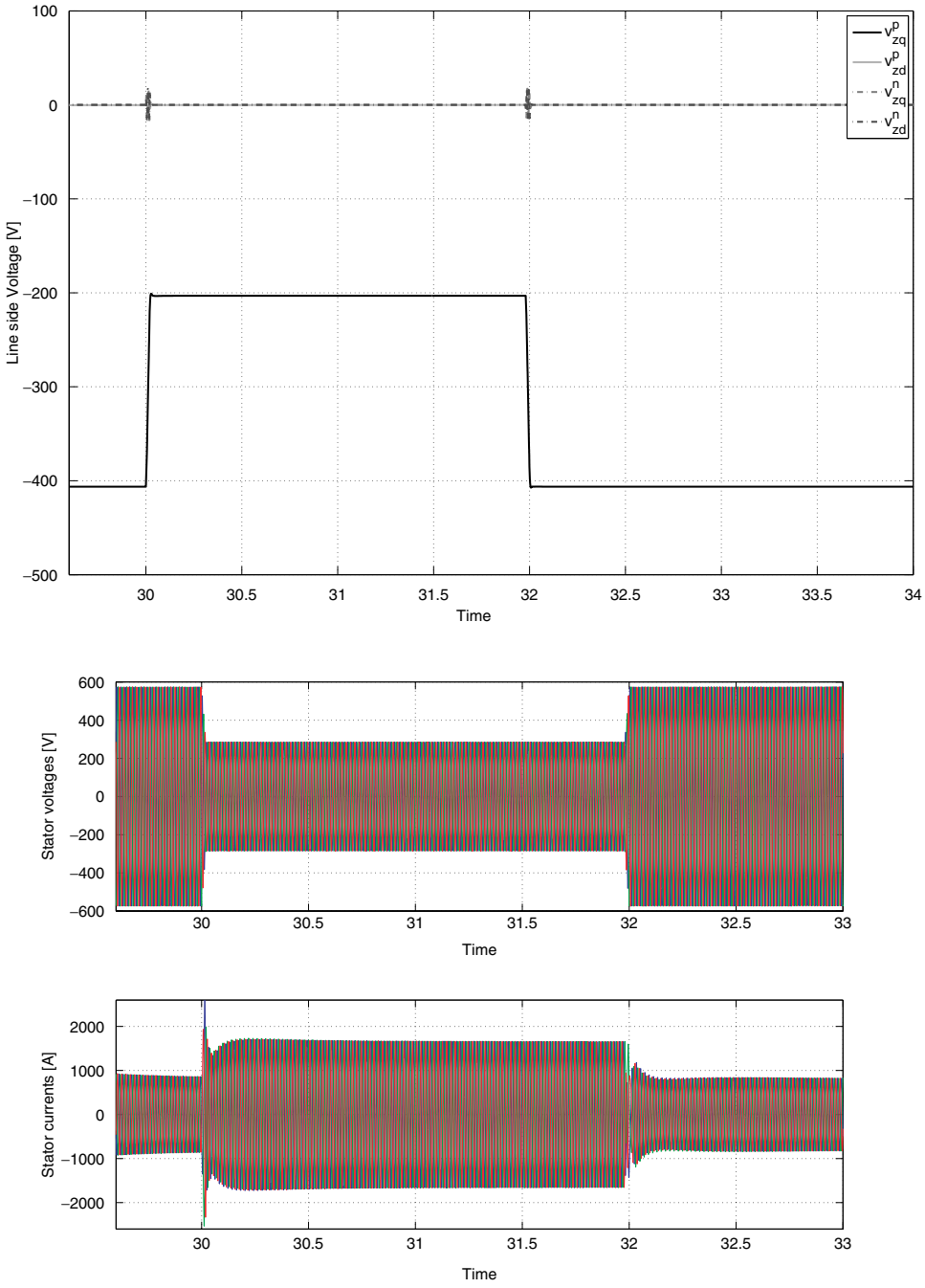


Fig. 28.10. Stator voltage in positive and negative sequence (top) and stator abc voltages and currents (bottom).

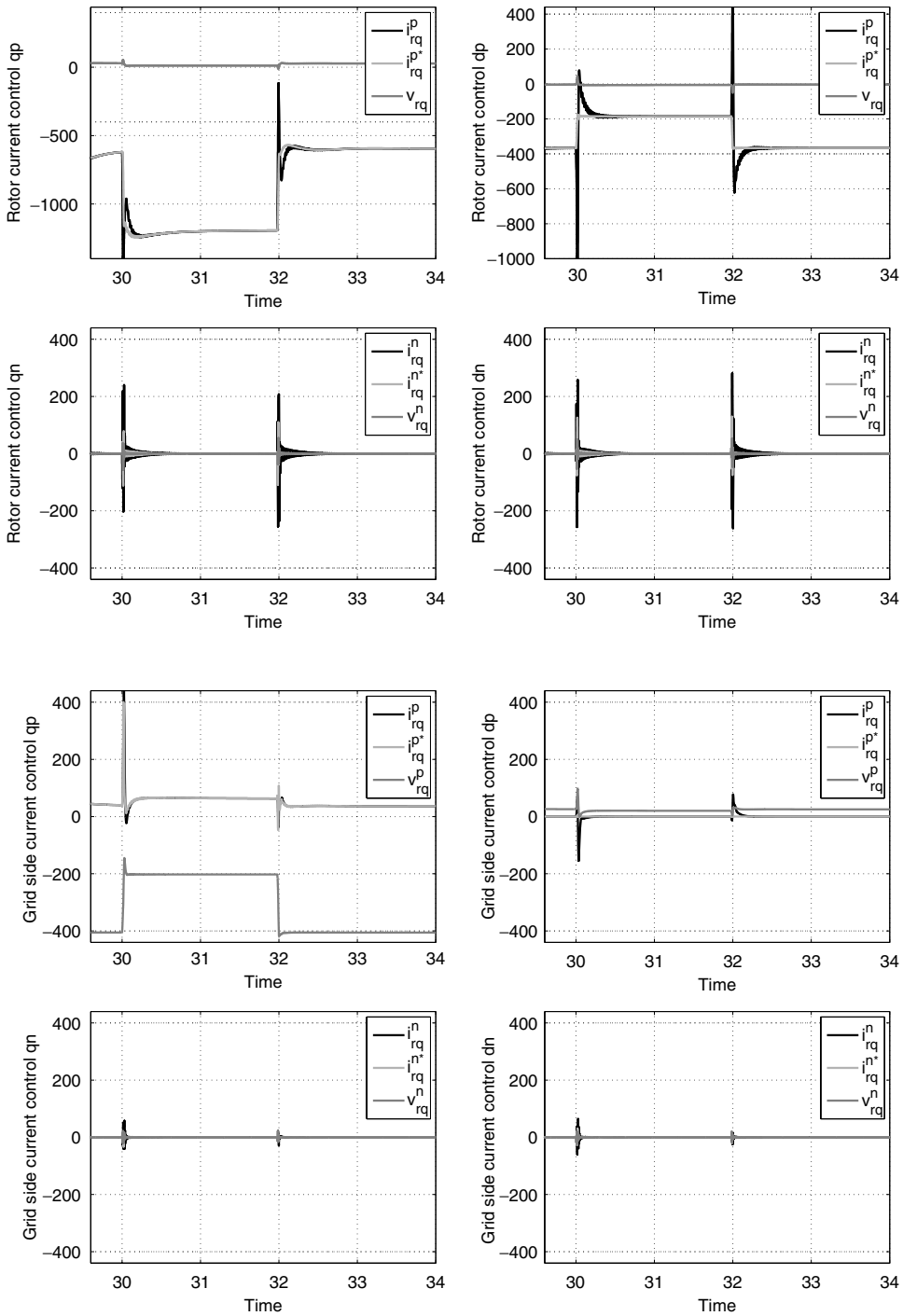


Fig. 28.11. Rotor-side and grid-side converter current loops.

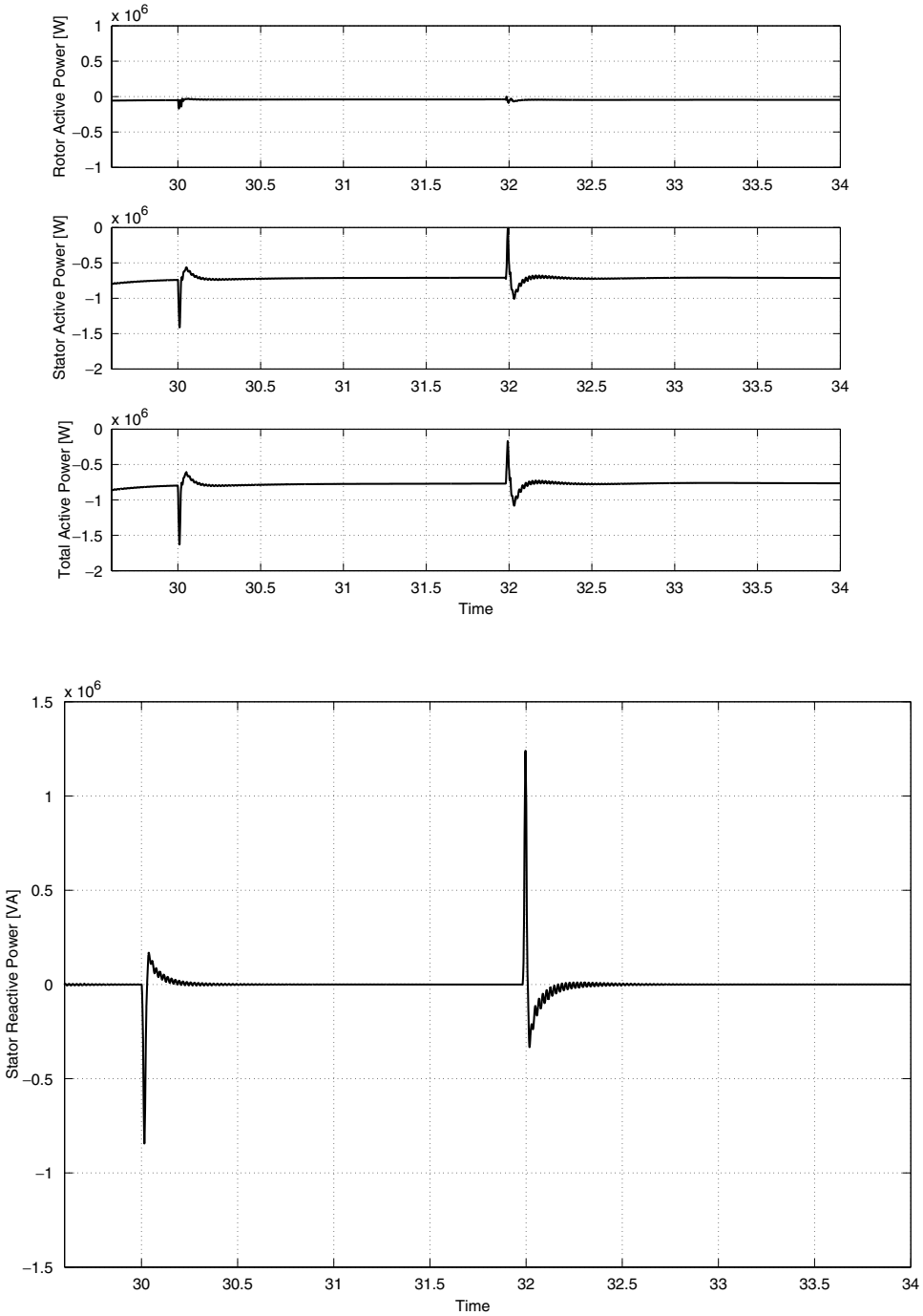


Fig. 28.12. Rotor, stator and total active power and stator reactive power.

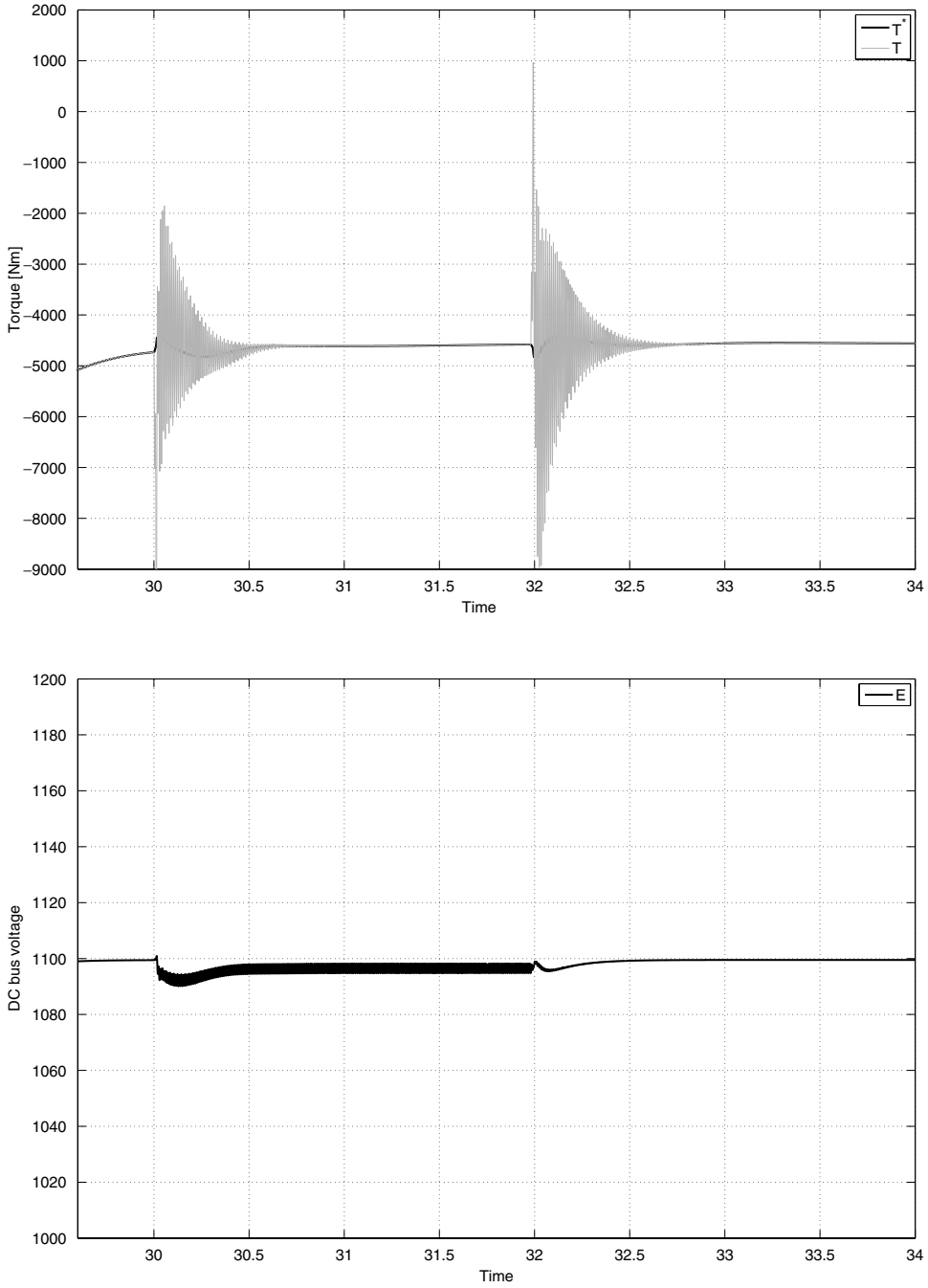


Fig. 28.13. Torque and DC bus response to an unbalanced voltage sag.

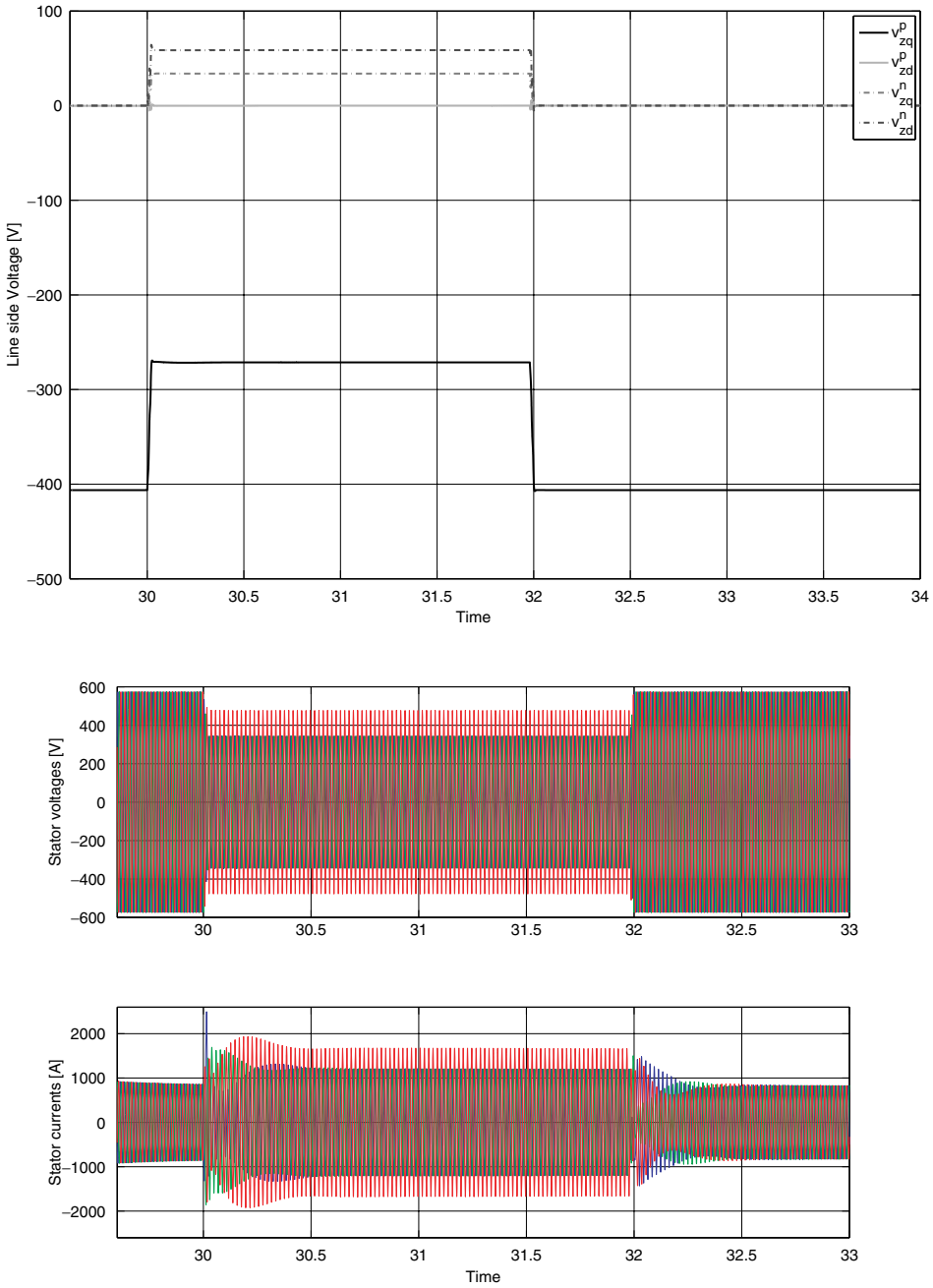


Fig. 28.14. Stator voltage in positive and negative sequence (top) and stator abc voltages and currents (bottom).

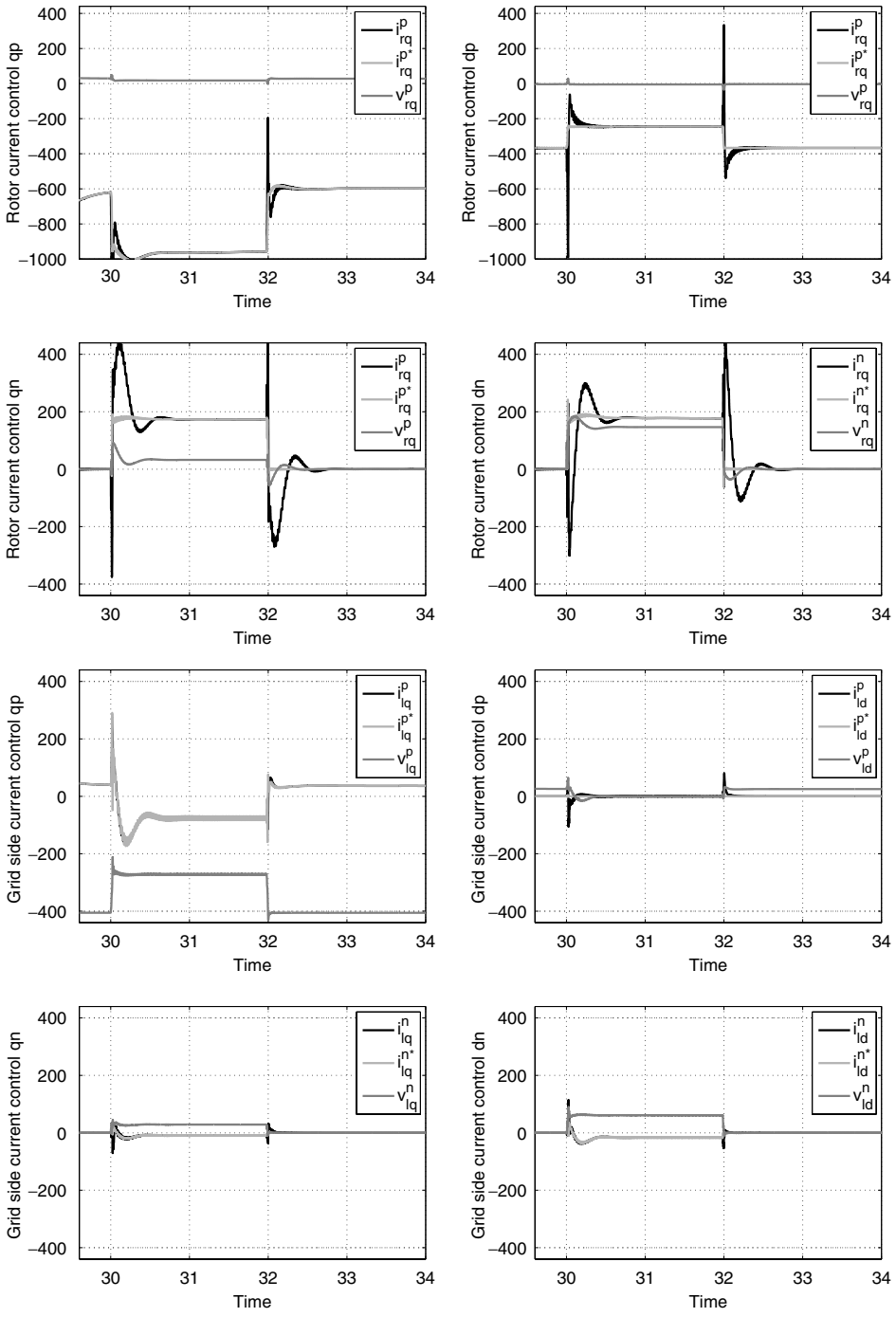


Fig. 28.15. Rotor-side and grid-side converter current loops.

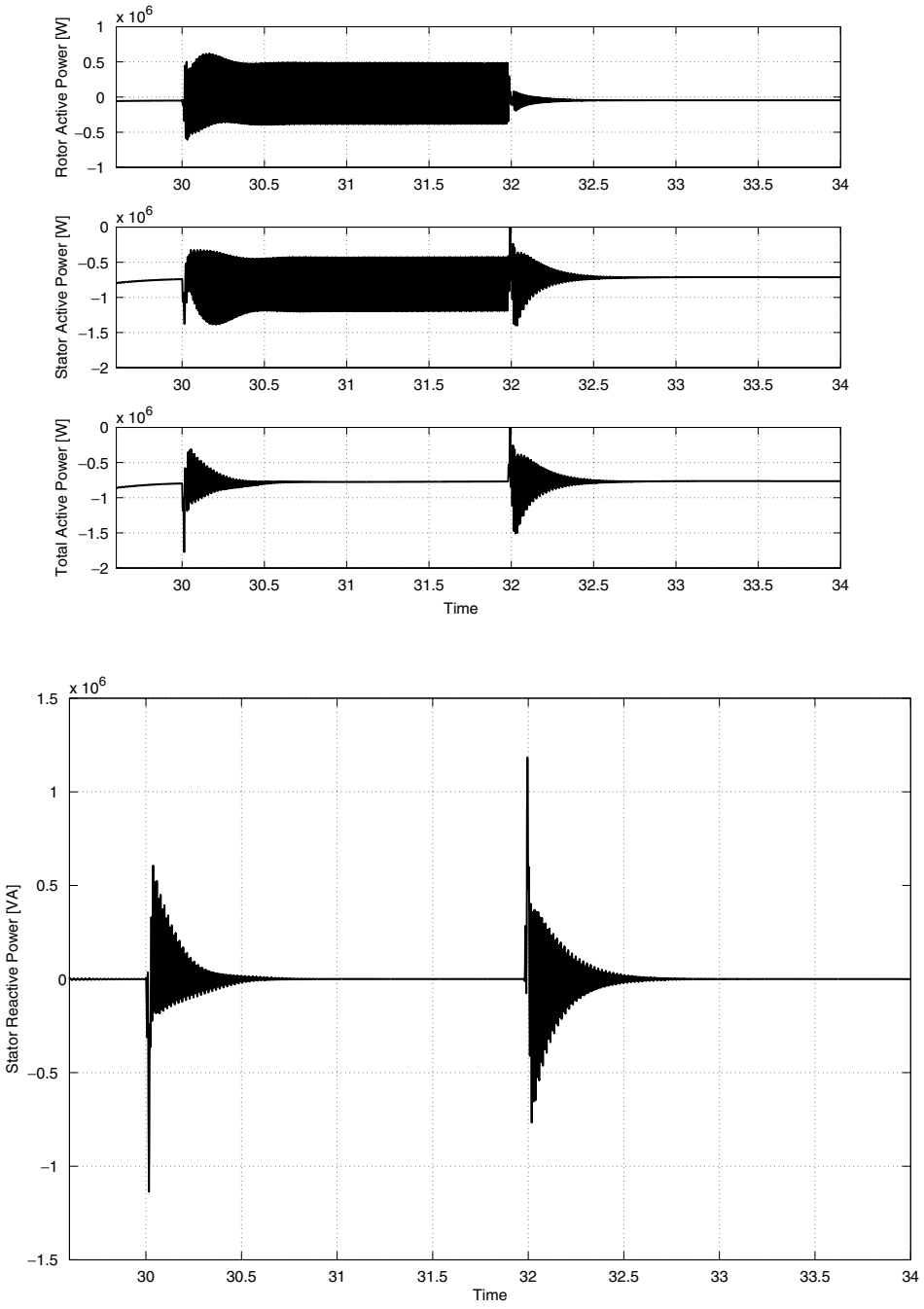


Fig. 28.16. Rotor, stator and total active power and stator reactive power.

### 28.6.1 *Balanced voltage sag*

A 50% voltage sag of 2 seconds have been applied when a 2 MW wind turbine was generating with a wind of 8.2 m/s.

The generator torque and DC bus voltage response are illustrated in Fig. 28.9. Stator voltages in positive and negative sequence along with abc stator voltages and currents are shown in Fig. 28.10. Rotor-side and grid-side converter current loops are shown in Fig. 28.11. Active and reactive powers are illustrated in Fig. 28.12.

### 28.6.2 *Unbalanced voltage sag*

A 50% voltage sag have been applied to two phases leaving the third phase undisturbed. The disturbance has been analyzed in a 2 MW wind turbine was generating with a wind of 8.2 m/s.

The generator torque and DC bus voltage response are illustrated in Fig. 28.13. It can be seen that although the inverse sequence provokes an oscillating flux, an almost constant torque can be achieved after a transient. The DC voltage response is shown in Fig. 28.13. As it has been stated, the constant torque implies oscillating rotor power which can be compensated with oscillating grid-side converter power. Using the proposed technique, the resulting DC bus voltage has minimized the oscillations.

The stator voltages in positive and negative sequence and the abc stator voltages and currents are illustrated in Fig. 28.14. Rotor-side and grid-side converter current loops are shown in Fig. 28.15.

Active and reactive power are illustrated in Fig. 28.16. It can be seen that while the total power (depending on the torque) is almost constant, stator and rotor active power are of oscillating nature.

## 28.7 Conclusions

The present chapter has presented presents a control technique for doubly fed induction generators under different voltage disturbances. The current reference are chosen in the positive and negative sequences so that the torque and the DC voltage are kept stable during balanced and unbalanced conditions. Both rotor-side and grid-side converters have been considered, detailing the control scheme of each converter while considering the effect of the crow-bar protection. The control strategy has been validated by means of simulations for balanced and unbalanced voltage sags.

## References

1. O. Gomis-Bellmunt, A. Junyent-Ferre, A. Sumper and J.Bergas-Jane, Ride-through control of a doubly fed induction generator under unbalanced voltage sags, *IEEE Transactions on Energy Conversion*. **23**, 1036–1045 (2008).
2. R. Pena, J.J.C. Clare and G. Asher, Doubly fed induction generator using back-to-back PWM convertersand its application to variable-speed wind-energy generation, *IEE Proceedings Electric Power Applications*. **143**(3), 231–241 (1996).
3. A. Junyent-Ferré, Modelització i control d'un sistema de generació elèctrica de turbina de vent. Master's thesis, ETSEIB-UPC, (2007).
4. L. Harnefors and H.-P. Nee, Model-based current control of ac machines using the internal model control method, *IEEE Transactions on Industry Applications*. **34**(1), 133–141 (Jan.–Feb., 1998). doi: 10.1109/28.658735.
5. A.D. Hansen and G.Michalke, Fault ride-through capability of DFIG wind turbines, *Renewable Energy*. **32**(9), 1594–1610 (July, 2007). doi: 10.1016/j.renene.2006.10.008.
6. J. Morren and S. de Haan, Ridethrough of wind turbines with doubly-fed induction generator during a voltage dip, *IEEE Transactions on Energy Conversion*. **20**(2), 435– 441, (2005). doi: 10.1109/TEC.2005.845526.
7. H.-S. Song and K. Nam, Dual current control scheme for PWM converter under unbalanced input voltage conditions, *IEEE Transactions on Industrial Electronics*. **46**(5), 953–959 (Oct., 1999). doi: 10.1109/41.793344.